ARTICLE IN PRESS

Extreme Mechanics Letters ▮ (▮▮▮▮) ▮▮▮–▮▮▮

Contents lists available at ScienceDirect

Extreme Mechanics Letters

journal homepage: www.elsevier.com/locate/eml

Miniaturized fracture experiments to determine the toughness of individual films in a multilayer system

R. Treml [a], D. Kozic [b], R. Schöngrundner [b], O. Kolednik [c], H.-P. Gänser [b], R. Brunner [b], D. Kiener [a,*]

[a] Department Materials Physics, Montanuniversität Leoben, Austria
[b] Material Center Leoben Forschungs GmbH, Leoben, Austria
[c] Erich Schmid Institute, Austrian Academy of Sciences, Leoben, Austria

GRAPHICAL ABSTRACT

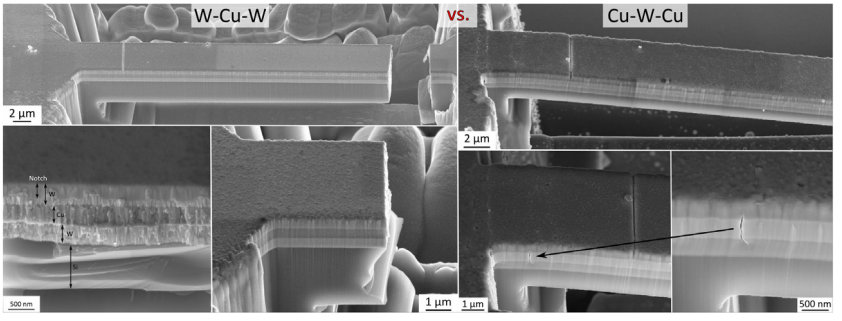

ARTICLE INFO

Article history:
Received 26 November 2015
Received in revised form 19 January 2016
Accepted 23 January 2016
Available online xxxx

Keywords:
Fracture toughness
Bending beam
Residual stress
Small scale mechanics
Multilayer
Finite element modelling

ABSTRACT

Recently, the miniaturization of devices in the field of microelectronics has become more and more important. This also implies an increased complexity of the devices, where multilayer thin film systems play a major role. The use of various material combinations leads to the development of residual stresses, potentially causing cracks. Therefore, to prevent failures a thorough understanding of material properties such as the fracture toughness at small scales is indispensable, as these may differ significantly from bulk values. In this study we use miniaturized fracture tests to investigate the fracture behaviour of Cu–W–Cu and W–Cu–W trilayer thin film systems, having a thickness of 500 nm per individual W or Cu layer. The films are subjected to differences in elastic properties and residual stress gradients that both influence the fracture behaviour and thus have to be included in all considerations. We demonstrate that for the W layers a valid *J*-integral can be evaluated. However, we find that the presented advanced treatment does not allow the

* Corresponding author.
E-mail address: daniel.kiener@unileoben.ac.at (D. Kiener).

http://dx.doi.org/10.1016/j.eml.2016.01.004

Please cite this article in press as: R. Treml, et al., Miniaturized fracture experiments to determine the toughness of individual films in a multilayer system, Extreme Mechanics Letters (2016), http://dx.doi.org/10.1016/j.eml.2016.01.004

extraction of valid fracture mechanical quantities for the Cu layers, pointing out the need to develop a more sophisticated approach for ductile materials.

1. Introduction

It is commonly known that the reliability of thin film systems in terms of the fracture behaviour is highly influenced by the mechanical properties of the films such as flow strength, Young's modulus, strength of the film–substrate interface, as well as the residual stress distribution in the film. When considering multilayer thin film systems, the situation gets more complicated as the combination of various materials increases, for example, the number of interfaces that can potentially fail. Moreover, the stacking sequence plays an important role as well [1], as it critically influences the residual stresses that develop. Additionally, it is worth mentioning that in small dimensions, especially for thin films, the above mentioned properties can differ significantly from their bulk values due to size effects that emerge from reduction of the grain size as well as the dimensional limitations of the reduced film thickness [2,3]. Therefore, as macroscale material data is not applicable anymore, miniaturized tests have to be applied to study the fracture behaviour at the small length scale [4–6], and for the material combination used in state of the art and future devices.

An established technique to determine the fracture toughness of (brittle) films is for example indentation [7,8], but with this method it is challenging to probe a single film, rather than measuring an apparent fracture toughness of the whole film–substrate composite. Therefore, it is more appropriate to determine single film properties by using more advanced small scale testing techniques such as pillar splitting [9], clamped cantilever bending, double cantilever bending, or single cantilever bending experiments [4,5,10]. Fracture experiments on bulk materials or single material thin films [6,11,12] using micro cantilevers have already been performed [10,13–15], but, up to now, not much attention has been paid to multilayer thin film systems [16,17]. However, with the ongoing miniaturization in microelectronics, the implementation of multilayer thin films rather than single films became more and more important, in terms of mechanical and electrical functionality.

In metallic film systems, the fracture mechanical treatment is governed by the size of the plastic zone in front of the crack tip. To apply linear elastic fracture mechanics (LEFM), the plastic zone size $r_{\mathrm{pl}} \propto K_{\mathrm{IC}}^2/\sigma_y^2$ has to be significantly smaller than the sample size and the crack length, with K_{IC} being the critical stress intensity for mode I fracture and σ_y the yield strength of the material. It can be expected that for ductile thin films r_{pl} will even reach the sample size, thereby requiring application of elastic–plastic fracture mechanics (E-PFM) and the J-integral to determine the crack driving forces [18,19]. To be able to determine correct data needed for the calculations, such as crack length and correct dimensions, in-situ experiments are preferably applied as demonstrated in [4,6,20].

It is known that a material inhomogeneity, such as an interface in a multi-layered system, can influence the crack growth drastically [21]. For instance, if a crack approaches an interface with a stiff/compliant transition ($E_{\mathrm{stiff}} > E_{\mathrm{compliant}}$) or a hard/soft transition ($\sigma_{y\,\mathrm{hard}} > \sigma_{y\,\mathrm{soft}}$), the crack extension is promoted, as the crack driving force is amplified. This is the so-called anti-shielding effect. On the other hand, a compliant/stiff interface ($E_{\mathrm{compliant}} < E_{\mathrm{stiff}}$) or a soft/hard interface ($\sigma_{y\,\mathrm{soft}} < \sigma_{y\,\mathrm{hard}}$) causes a shielding effect, which retards the crack when approaching the interface, as the effective crack driving force is lowered. As long as the plastic zone around the crack tip does not touch the interface, which is the case for small loads, the influence of the Young's modulus is most significant. As the load is increased and the plastic zone extends into the next layer, the impact of the change in yield strength gains more importance. A third contribution to the effective crack driving force comes from the influence of the hardening parameter, but as this influence is negligible compared to that of Young's modulus and yield strength, it is not discussed here. In conclusion, the fracture resistance can be highly improved by engineering the layered structure based on the knowledge of Young's modulus, the material flow behaviour and tailored residual stresses [22–24].

In this work, the fracture behaviour of copper (Cu) and tungsten (W) multi-layer thin film systems that are subjected to residual stresses with pronounced gradients [25] is investigated under mode I loading. Therefore, we perform a combination of miniaturized fracture experiments in-situ in the scanning electron microscope (SEM) accompanied by finite elements (FE) simulations in order to assess the validity of different fracture mechanical concepts when applied to such complex small scale systems.

2. Experimental

In the current paper two different stacking configurations of alternating Cu and W layers, namely Cu–W–Cu on Si and W–Cu–W on Si (100), were investigated. The Cu and W films were prepared via physical vapour deposition with a thickness of approx. 500 nm per layer. The grains are almost globular with a grain size ranging from 60 to 70 nm. For a detailed description of the deposition conditions and the material characterization, the reader is referred to a previous work [25].

As already mentioned, the residual stresses stored in such thin film systems may play a crucial role for the fracture behaviour. Therefore, the depth resolved residual stress profiles of the two systems were assessed using the ion beam layer removal (ILR) method [25–27] for the trilayer systems deposited on a Si (100) wafer with

Please cite this article in press as: R. Treml, et al., Miniaturized fracture experiments to determine the toughness of individual films in a multilayer system, Extreme Mechanics Letters (2016), http://dx.doi.org/10.1016/j.eml.2016.01.004

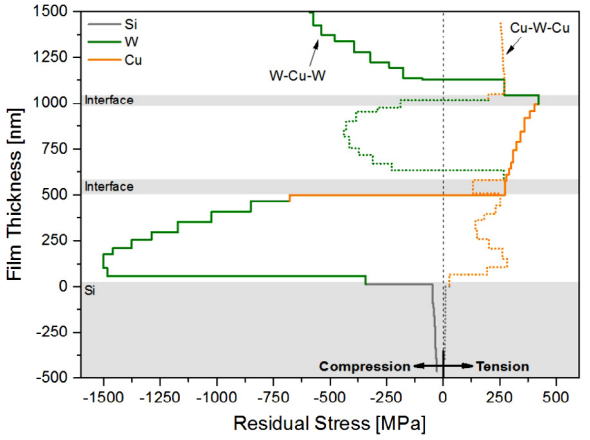

Fig. 1. Residual stress profiles of Cu–W–Cu (dashed line) and W–Cu–W (continuous line) on Si (100).

a thickness of 525 μm. The underlying principle of the method is that the residual stress can be calculated from the deflection of the cantilever, which originates from a combination of the residual stress and the stress caused by the deformation of the cantilever from cutting it free. If parts of the film are removed, the load caused by the remaining residual stresses changes, as well as the stiffness of the beam. Therefore, the resulting stress in the cantilever changes for the remainder of the film and since the stiffness is known, the residual stress profile can be calculated from the deflection profile [25]. The residual stress profiles for the two systems are depicted in Fig. 1. The two samples exhibit almost constant tensile residual stresses for the Cu layers and compressive stresses with pronounced stress gradients for W layers. As the films are deposited at room temperature only growth stresses evolve, which develop due to the differences in materials parameters and deposition conditions. As focused ion beam milling is the tool for these experiments, a point of concern is whether the Ga ion impingement alters the residual stresses or not. In [25] it was already shown that the deflection of the beam does not change anymore when all the deposited film is removed and only Si is milled. Based on this findings we conclude, that an influence from the ion beam can be neglected for the present study. For more details concerning the determination and interpretation of the stress profiles, the reader is referred to [25].

2.1. Sample preparation

Micro cantilevers were prepared to investigate the fracture properties of the thin multilayer films subjected to residual stresses. First, a lamella with a width of 20–30 μm is prepared using a Hitachi-E3500 Cross Section Polisher (Hitachi, Tokyo, Japan). With this method all material that is not covered by a mask is removed by low energy Ar ions [28]. The final cantilevers are produced in a LEO 1540XB focused ion beam (FIB) workstation (Zeiss, Oberkochen, Germany). In a first step, the coarse shaping of the cantilever is done from the top and the side with an ion beam current of 1–5 nA. Then the notch is cut using

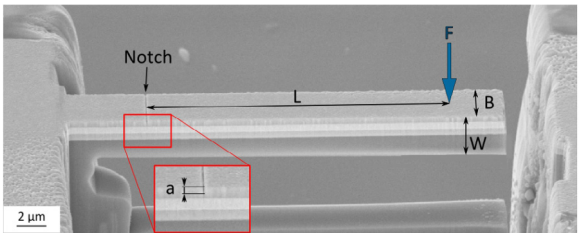

Fig. 2. Secondary electron micrograph of a FIB prepared Cu–W–Cu fracture sample with a notch. Dimensions for later analysis are indicated.

Table 1
Dimensions of the tested cantilevers. For the notched samples, L is defined as the length between the indenter tip and the crack in the W layer, while for S1, S2, and C1-3 it refers to the distance between indenter and site of failure. B is the sample width, W the sample height and a the crack length.

System	Sample no.	L (μm)	B (μm)	W(μm)	a (nm)
W–Cu–W	S1	24.7	6.5	4.3	–
	S2	29.6	4.6	4.6	–
	S3	20.5	3.8	4.0	437
	S4	22.5	3.3	5.6	445
	S5	24.0	4.4	4.5	380
	S6	20.1	5.1	4.6	344
Cu–W–Cu	C1	24.9	5.2	2.5	Unknown
	C2	21.9	4.1	4.5	Unknown
	C3	23.7	4.8	4.3	Unknown
	C4	19.1	3.6	4.3	500

the line milling mode for all samples except W–Cu–W samples S1 and S2. A milling time per length of approx. 0.9–2 s/μm for the milling line and an ion current of 50 pA are used. The actual cutting time depends on the desired depth of the notch and the sputter rate of the material to be notched. Subsequently, the side and bottom of the cantilever are polished with an ion current of 500 pA. With this final polishing of the side surfaces, the curtaining effect from notching is removed and a constant notch depth over the beam width is reached simultaneously with a smooth surface. The dimensions of the cantilevers tested in this work are given in Table 1, and an image of a representative Cu–W–Cu fracture sample with all relevant annotations is displayed in Fig. 2.

2.2. Fracture experiments

The experiments were performed in-situ in a LEO 982 SEM (Zeiss, Oberkochen, Germany) using an UNAT-SEM Indenter (ASMEC, Radeberg, Germany) with a wedge-shaped conductive diamond tip (Synton-MDP AG, Nidau, Switzerland) [29]. All experiments were performed in a displacement controlled mode with a loading and unloading speed of 1 μm/min, respectively. During the test, the displacement and force were recorded at 64 Hz and scanning electron (SE) micrographs were taken automatically using a frame grabber at a frame rate of 1 fps, enabling a detailed view on the deformation process and the crack growth for later analysis. Each sample was loaded and unloaded several times with increasing displacement amplitude. From these experiments a critical force F_c was determined for every load–displacement curve, either

Please cite this article in press as: R. Treml, et al., Miniaturized fracture experiments to determine the toughness of individual films in a multilayer system, Extreme Mechanics Letters (2016), http://dx.doi.org/10.1016/j.eml.2016.01.004

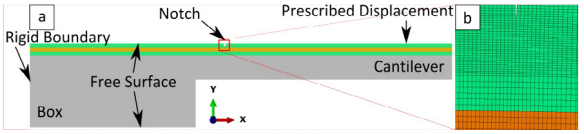

Fig. 3. (a) Model used for simulation with a zoom into the notch area in (b).

Table 2
Material parameters used for the FE simulation [33–36].

	E (GPa)	ν (–)	σ_y (GPa)	m (–)
Cu	130	0.34	0.989	4.4
W	411	0.28	1.970	14.3
Si	170	0.28	–	–

before a load drop occurred, which is equivalent to a crack extension, or at maximum load.

3. Finite element simulations

An FE study using ABAQUS (Simulia, Dassault Systems Simulia Austria GmbH) was performed to calculate the J-integral for different crack lengths of both layered systems, intended to determine the fracture toughness of the W and the Cu films.

To this purpose, a two dimensional micro cantilever (see Fig. 3) was modelled according to the geometries used in the experiments (Table 1) and the materials properties listed in Table 2.

The yield and hardening behaviour for the W and the Cu layer were identified from spherical nanoindentation experiments [30], performed using a constant loading rate on a G200 nanoindenter (Keysight Tec. Inc., Santa Rosa, CA, USA). The yield strength σ_y and the inverse hardening parameter m for W and Cu were determined by means of inverse modelling, assuming a Ramberg–Osgood material model [31,32]:

$$\varepsilon = \frac{\sigma}{E} + a\left(\frac{\sigma}{\sigma_y}\right)^m. \tag{1}$$

Here, ε is the total strain and σ is the incrementally increasing stress. The value of the yield offset a is 0.2%, a typical value for metals, and the fit parameters are the inverse hardening parameter m and the yield strength σ_y. The results are given in Table 2 and for more details concerning the calculation procedure the reader is referred to Appendix A.

Eight-node full-integration biquadratic plane strain elements (CPE8) were used for discretization of the fracture beams. The position of the crack tip in relation to the interface determines the resolution of the mesh, since there has to be a sufficient number of elements between interface and crack tip in order to compute reliable J-integral values. To validate the sufficiency of the number of used elements in front of the crack tip, we have performed a convergence test with various mesh sizes. The test shows that the J-integral yields reliable results for a mesh size of >5 elements in front of the crack tip, while 10 elements were used here. The back of the beam is connected to a generated box by a "tie condition", to resemble the untreated environment around the specimen. The top of the box is unconstrained to simulate a free surface condition, while the back is clamped. The bottom of the box is also unconstrained in order to simulate the compliance of the used experimental setup. Crack length and position are determined from high resolution SEM images taken at maximum loading. Loading of the specimens in the simulation is done force controlled. The load is taken from the experimental force–displacement curves and is equal to the maximum load either before a significant load drop occurs or after the crack has extended to a certain length.

As a first step the locally resolved residual stresses for the thin film system are implemented as an initial condition via the user subroutine SIGINI implemented in ABAQUS. The code applies the determined residual stresses (see Fig. 1) over the thickness of the layer structure. Notably, the initial residual stresses applied to the micro cantilever were determined for a constrained film on a 525 μm Si substrate [25]. Therefore, the residual stresses have to be relaxed in order to reflect the state after the beam has been cut free in the experiment. The cantilever experiences a slight displacement in loading direction after an equilibrating step for the residual stress. The change of the residual stress distribution due to this relaxation is depicted in Fig. 4 for both systems.

As second step the crack driving forces are calculated as a contour integral around the crack tip using the J-integral concept [18] with the ABAQUS virtual crack extension method. The fracture toughness is then calculated from the following equation, which is notably only valid for linear elastic fracture mechanics:

$$K_J = \sqrt{J\frac{E}{1-\nu^2}}, \tag{2}$$

with E being the Young's modulus and ν the Poisson's ratio.

To demonstrate the applicability of the J-integral, the stress perpendicular to the crack propagation direction is plotted against the increasing distance from the crack tip for the samples W–Cu–W S3–S5 in Fig. 5. Here, the regime where the slope of the curves resembles a $1/\sqrt{r}$ behaviour of the stress, which is required to follow the K approach, is not existent. Nonetheless, roughly about 10 nm away from the crack tip until close to the interface, a J-dominated zone is built up [37], as evident in Fig. 5 where the stress decreases with a constant slope, thus the J-integral is path independent.

4. Analysis and results

4.1. Fracture experiments on W–Cu–W

First the two samples W–Cu–W S1 and S2 without a notch were tested to estimate the fracture stress. The corresponding force–displacement data of S1 is depicted in Fig. 6 and a supplementary online video is available for this test (see Appendix C). The top W layer fractures in the first test cycle T1 and the crack stops at the interface W/Cu. The stiffness of the beam decreases due to the crack extension, which is shown by the fact that the slope of the unloading segment is significantly smaller than that of the

Please cite this article in press as: R. Treml, et al., Miniaturized fracture experiments to determine the toughness of individual films in a multilayer system, Extreme Mechanics Letters (2016), http://dx.doi.org/10.1016/j.eml.2016.01.004

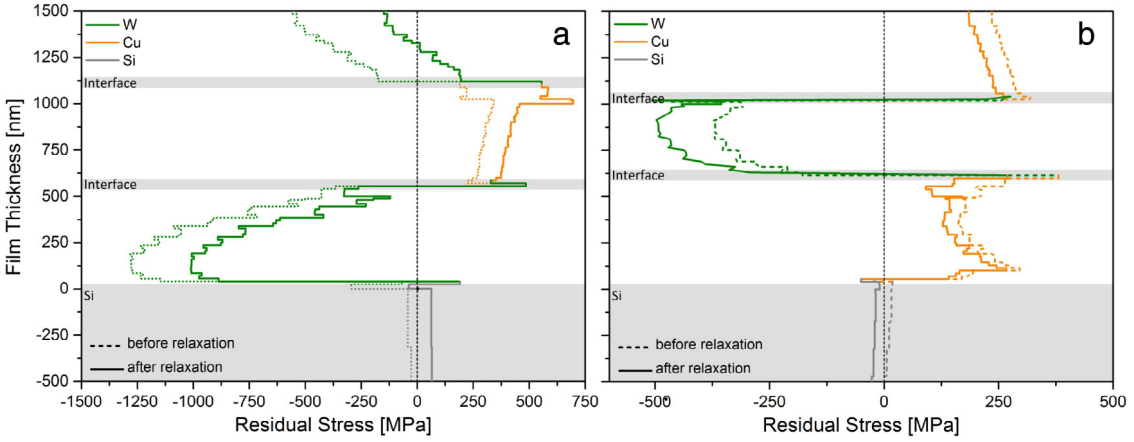

Fig. 4. Residual stress profiles for W–Cu–W (a) and Cu–W–Cu (b) before and after the relaxation of the beam.

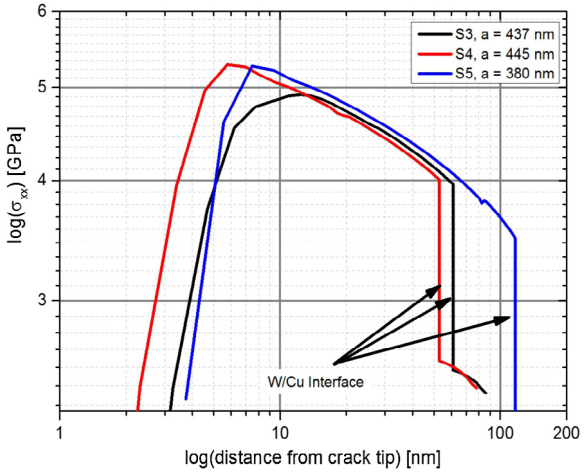

Fig. 5. Stress perpendicular to the crack propagation direction for W–Cu–W in dependence of the increasing distance from the crack tip for three samples. (For interpretation of the references to colour in this figure legend, the reader is referred to the web version of this article.)

loading segment. In the second test cycle T2, only a crack tip blunting in conjunction with a possible crack extension in the Cu layer can be observed, again leading to a reduction in stiffness and a lower slope for the unloading step. In the third test cycle T3 ultimate fracture through the second W layer and the Si substrate occurs. The fracture stress σ_{fr} is calculated as the maximum surface stress from simple beam theory using Eq. (3) [12]:

$$\sigma_{fr} = \frac{6FL}{BW^2}. \tag{3}$$

The calculated values are 2.5 GPa and 2.9 GPa for S1 and S2, respectively.

To determine the fracture toughness, the following samples S3–S5 were notched to different depths. The fracture experiment for sample S5 is depicted in Fig. 7. The data of testing cycles T4 to T6 is shifted to the right to make the influence of crack propagation on the force–displacement data better visible. The inset in Fig. 7(a) as well as (b) are taken before the test. Fig. 7(g) is taken after the test, the images of test cycles T3 to T6 (Fig. 7(c)–(f)) were taken at maximum load of the individual loading step. The initial notch has a length of 380 nm in the top W layer. In test cycle T3 the remaining W ligament breaks, the crack propagates unstably, but then stops right after the interface W/Cu. For the following test cycles T4 and T5 only a crack tip blunting with little crack propagation in the Cu layer is visible. At a maximum load of 1.67 mN the remaining Cu layer, the bottom W layer and the Si substrate break. Fig. 8(a) and (b) show inclined views of the fracture surfaces of the two layer systems with indications for the notch and the single layers, respectively. For both systems intergranular fracture is observed.

4.2. Comparison of experiment and simulation

In Fig. 9, the experimental and the simulated load–displacement curves for W–Cu–W S3 are compared. From the slope of the elastic simulation (blue line) it is obvious, that a linear elastic modelling of the cantilever does not match the experiments. It is evident from the experimental curve that under higher loads the materials undergo plastic deformation. By using the yield strength and hardening parameter determined from nanoindentation experiments the simulated and experimental loading curves are in good agreement, as shown by the red and green lines in Fig. 9. In the presence of residual stresses the curve (green) shows a flatter behaviour, reaching the yield point before the loading curve (red), where the residual stresses are omitted.

4.3. Calculation of stress intensity factors

To demonstrate the influence of the stacking order on the crack driving forces in a thought experiment, the stress intensity factor K is calculated for various crack lengths for the layered systems W–Cu–W and Cu–W–Cu, as well as for a single Cu and W layer. That means that the calculated K-factors do not display a real experiment, but the behaviour of the stress intensity factor for a crack extending under a constant load. Although this is intended as a thought experiment, to get somewhat

Please cite this article in press as: R. Treml, et al., Miniaturized fracture experiments to determine the toughness of individual films in a multilayer system, Extreme Mechanics Letters (2016), http://dx.doi.org/10.1016/j.eml.2016.01.004

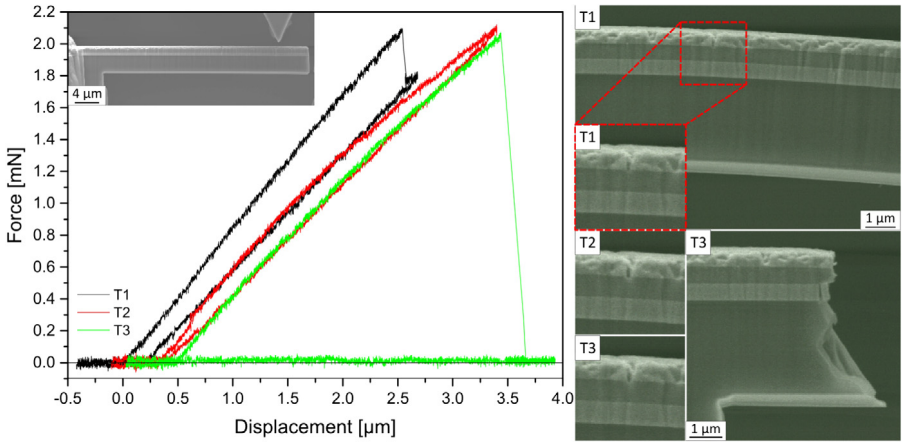

Fig. 6. Force–displacement data for three consecutive loading steps of the unnotched W–Cu–W sample S1 including SE images of the specimen at maximum load or after fracture, respectively.

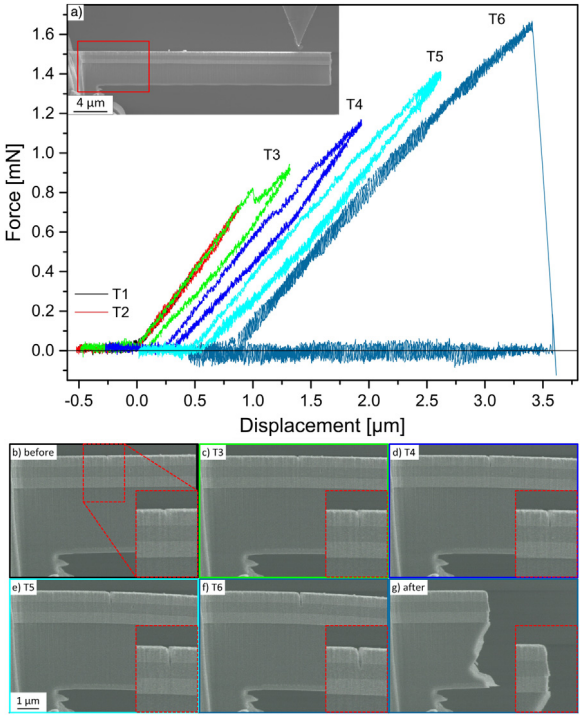

Fig. 7. (a) SE micrograph of the specimen with the indenter before the test and force–displacement curves of the W–Cu–W specimen S5 showing the test cycles T1–T6. Red rectangle shows the zoom-in region. (b–g) SEM images before (b) and after (g) the test, and at maximum load for loading steps T3–T6 (c–f). The crack is shown magnified in the inset. (For interpretation of the references to colour in this figure legend, the reader is referred to the web version of this article.)

realistic values, for the W–Cu–W system the load is taken from Fig. 6 right before the significant load relief in the first loading cycle T1. For the Cu–W–Cu system the force before fracture of the middle W layer in sample C3 is used. The stress intensity factors are calculated using Eq. (2) and the results are plotted in Fig. 10. The interface Cu/W (compliant/stiff) clearly provides a shielding effect, whereas the interface W/Cu (stiff/compliant) leads to an anti-shielding effect [38]. In all W layers, K has a steep slope rising towards the next interface, whereas the curve is rather flat for the Cu layers. It is demonstrated that the layered structure in comparison to a single Cu (dashed grey line) or W (dashed black line) film with the same thickness, has a high influence on the crack driving force. In case of a single film, K would rise continuously with a square root dependency. However, for both multilayer systems at the transition between the two materials large discontinuities are shown, which are dependent on the stacking order. In addition, it is demonstrated that the influence of the layered structure, and thus the change in Young's modulus, on the stress intensity factor is more pronounced than the influence of the residual stresses. Furthermore, the effect from the residual stresses contributes only between 0.1% and 10% to the stress intensity factor once load is applied, depending on the crack tip position. Thus, in this configuration, the major part of the stress intensity factor comes from the external load.

5. Discussion

Up to now, the fracture toughness for such miniaturized samples was most often calculated using LEFM to determine critical K-values. The rational for this was of course that for rather low toughness materials the plastic zone is reasonably small compared to the sample size [10–12,39,40]. However, in the presented multilayer samples, additionally the change in elastic properties across the interfaces and the residual stress distribution have to be taken into account. Furthermore, the fact that all samples are loaded stepwise could lead to the evolution of a cyclic plastic zone in copper. To rule this out, the W–Cu–W sample S6 was tested in a single loading to failure and it was shown that there is no difference in the materials response compared to all other samples. Details concerning this test are described in Appendix B.

In the case of an elastic–plastic material behaviour of the layer system we have verified that we can calculate the crack driving forces with E-PFM, see Fig. 5. In Fig. 11 the crack driving forces for the samples W–Cu–W S3–S5 are shown. The maximum force for the first crack extension

Please cite this article in press as: R. Treml, et al., Miniaturized fracture experiments to determine the toughness of individual films in a multilayer system, Extreme Mechanics Letters (2016), http://dx.doi.org/10.1016/j.eml.2016.01.004

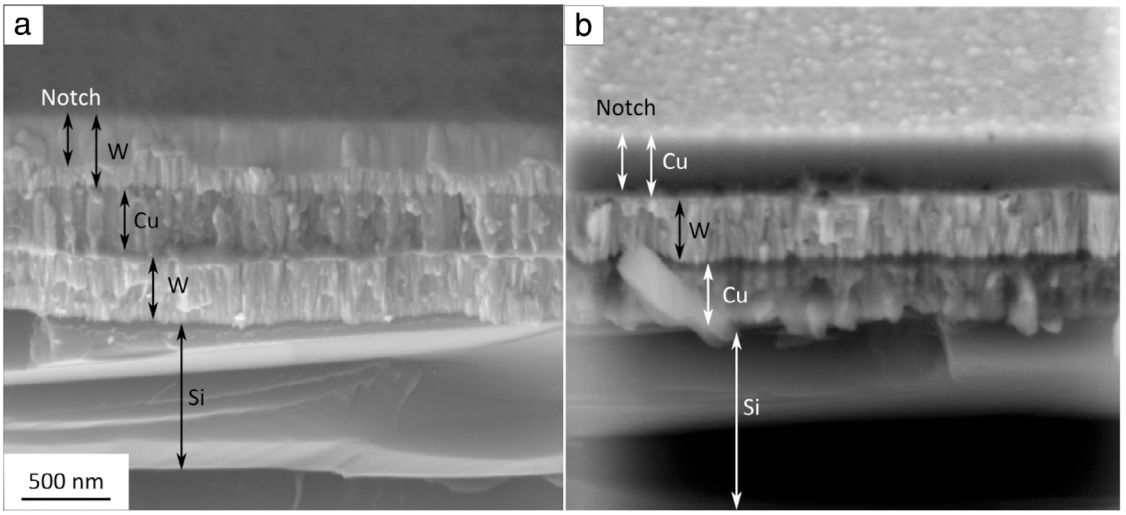

Fig. 8. SE micrographs showing the stack, the initial notch and the fracture surface under 45° stage tilt for samples W–Cu–W S5 (a) and Cu–W–Cu C4 (b).

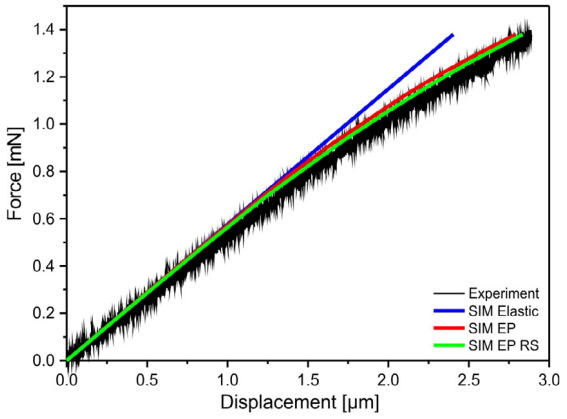

Fig. 9. Experimental and simulated (SIM) force–displacement curves for W–Cu–W S3 including elastic, elastic–plastic (EP), and EP material behaviour with and without residual stresses (RS). (For interpretation of the references to colour in this figure legend, the reader is referred to the web version of this article.)

(T3) is equal to the force at which a load drop in test T3 occurs, breaking through the W-layer. For the second (T4) and third (T5) crack extension the maximum load is equal to the force before unloading the cantilever. For the fourth crack extension (T6) the force is equal to the load when the whole specimen breaks.

As a first approximation, the experimental data of the W–Cu–W system is evaluated with Eq. (4), with $f(a/W)$ taken from [6].

$$K = \frac{FL}{BW^{3/2}} f\left(\frac{a}{W}\right), \tag{4}$$

where

$$f\left(\frac{a}{W}\right) = 4\frac{\left\{3\left(\frac{a}{W}\right)^{0.5}\left(1.23 - \left(\frac{a}{W}\right)\left(1 - \left(\frac{a}{W}\right)\right)\right)\left(-6.09 + 13.96\left(\frac{a}{W}\right) - 14.05\left(\frac{a}{W}\right)^2\right)\right\}}{2\left(1 + 2\left(\frac{a}{W}\right)\right)\left(1 - \left(\frac{a}{W}\right)\right)^{1.5}}.$$

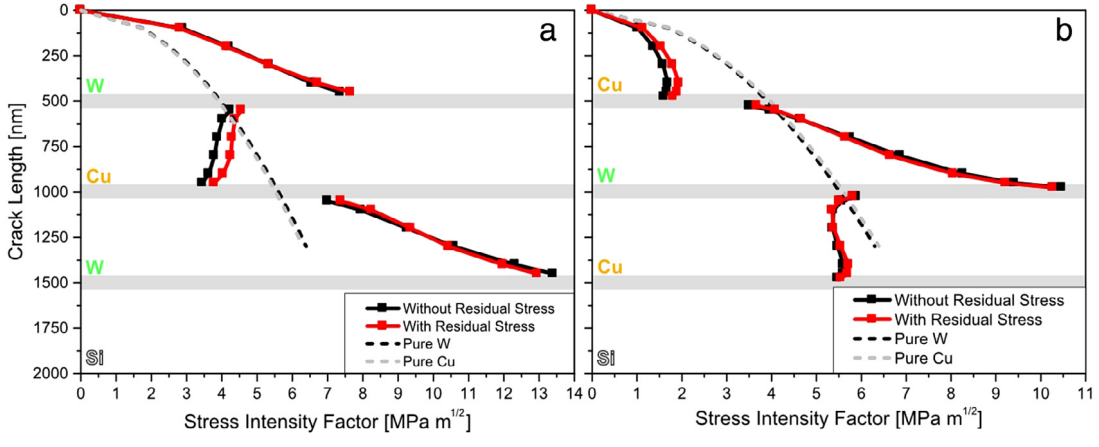

Fig. 10. Stress intensity factors vs. crack length for W–Cu–W (a) and Cu–W–Cu (b). The continuous line would be the expected behaviour for homogeneous W or Cu films.

Please cite this article in press as: R. Treml, et al., Miniaturized fracture experiments to determine the toughness of individual films in a multilayer system, Extreme Mechanics Letters (2016), http://dx.doi.org/10.1016/j.eml.2016.01.004

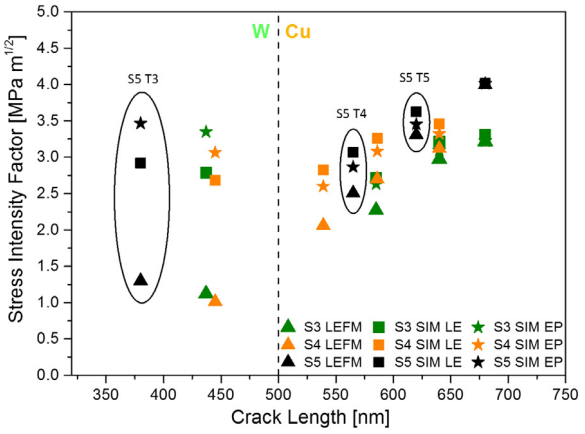

Fig. 11. Stress intensity factors for different crack lengths S3–S5 for the system W–Cu–W, calculated by applying linear elastic fracture mechanics (LEFM) and simulating linear elastic (LE) or elastic–plastic (EP) material behaviour. (For interpretation of the references to colour in this figure legend, the reader is referred to the web version of this article.)

This equation assumes a homogeneous material for the cantilever. The results of this linear elastic approach are shown in Fig. 11 as triangles. As demonstrated here, this does not give satisfying results compared to the FE calculations which include material properties, layer structure and residual stresses (rectangles and stars).

In a second approximation, the J-integral values are calculated from an FE analysis of the loaded fracture cantilevers, assuming a linear elastic material behaviour (rectangles). The determined J-values are converted to K using Eq. (2).

As a third approximation the J-integral is evaluated for an elastic–plastic material behaviour determined from nanoindentation experiments (Table 2), shown as stars. Again, the determined J-values are converted to K using Eq. (2). As predicted in Fig. 10, for the cracks in the top W layer the anti-shielding effect of the stiff/compliant W/Cu interface causes the significant increase of K relative to the result from Eq. (4). As the crack propagates into the Cu-layer, the anti-shielding effect diminishes and the shielding effect from the second Cu/W interface gets more pronounced (see Fig. 10(a)), thus the difference between the K values from the three calculations shrinks. In Fig. 11 we also see differences between the FE calculations with linear elastic (rectangles) and elastic–plastic (stars) material behaviour. The EP value of S5 T3 is higher than the linear elastic result. This can be explained by an additional anti-shielding effect from the hard/soft transition at the W/Cu interface. For the crack extension in S5 T4 and T5 in the Cu-layer a lower value of the crack driving force compared to the linear elastic calculation is obtained. The reason for this is a shielding effect of the soft/hard Cu/W interface. In the Cu-layer the extent of the plastic zone in front of the crack tip reaches the Cu/W interface. As a consequence, it is not possible to determine critical stress intensity factors for the Cu layers with the current approach. These findings are consistent for all samples S3–S5. For the top W layer a critical stress intensity factor of 2.8 ± 0.1 MPa$\sqrt{\text{m}}$ was calculated for the linear elastic material behaviour, whereas for the elastic–plastic behaviour the value is 3.3 ± 0.2 MPa$\sqrt{\text{m}}$ These values can be compared to the work of separation converted to a K value, which is approx. 1.6 MPa$\sqrt{\text{m}}$ for W [41]. The values calculated in this work are of course higher, as the material possesses defects that lead to an energy dissipation by plastic deformation before failure. When looking into literature, we find K_{IC} values in the range from 1 to 2.5 MPa$\sqrt{\text{m}}$ [35] for magnetron sputtered W thin films. However, the authors did not state the grain size and residual stress state in their films. If they had tensile residual stresses present in the films, but not accounted for them in their calculation, the resulting K value turns out lower compared to the present results, explaining the discrepancy.

When looking at the inverse system Cu–W–Cu, even more problems arise regarding the ductility of Cu concerning the calculation of fracture toughness values. For samples C1 to C3 the W layer failed between the notch and the fixation, whereas the Cu layers are just deformed (see supplementary video 2, Appendix C). For an imperfect sample geometry and internal defects this can be explained by looking at Fig. 10(b). Here, we see that the stress intensity factor for the W layer is much higher than for the two Cu layers. Thus, internal failure of grain boundaries under load, considering that the fracture surface is intergranular (see Fig. 8), would be more critical in the W layer than within the Cu layers. Only with notching almost the whole top Cu layer and reducing the distance between notch and fixation, it was possible to break the cantilever rather than only the inner W layer. Due to the extended amount of plasticity in this system, our current approach is not valid, and more sophisticated treatments such as the configurational force concept [21,38,42,43] may be applicable. Nevertheless, from the phenomenological point of view we emphasize that the system Cu–W–Cu is highly interesting regarding mechanical failure of devices, as the Cu layers act as perfect crack arrestor (see supplementary video 2, Appendix C). Thus, for example by altering the number of layers, the stacking sequence and the individual layer thickness, the capacity of prohibiting crack propagation can be improved [44,45].

6. Conclusion and outlook

In this study we performed miniaturized fracture experiments on Cu–W–Cu and W–Cu–W trilayers on a Si (100) substrate in-situ in the SEM. Subsequently, the resulting mechanical data was used as input data for the FE simulation taking into account the elastic–plastic material behaviour and the residual stresses. With this analysis we could demonstrate the influence of a stressed layered structure on the crack driving forces. Within the current approach we are able to determine valid fracture toughness values for the top W layers. Regarding the Cu layer, we observe that it acts as crack arrestor in such layered systems due to its ductility and rather low Young's modulus. Unfortunately, this positive effect at the same time complicates evaluation of a valid fracture quantity for the Cu layers using the present methodology. In the future, determining the fracture toughness of such ductile interlayers should be addressed by the configurational force concept.

Please cite this article in press as: R. Treml, et al., Miniaturized fracture experiments to determine the toughness of individual films in a multilayer system, Extreme Mechanics Letters (2016), http://dx.doi.org/10.1016/j.eml.2016.01.004

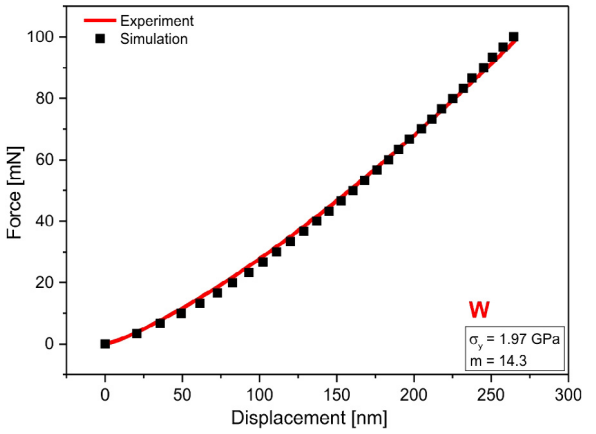

Fig. A.1. Experimental and fitted nanoindentation force–displacement curve for a W film.

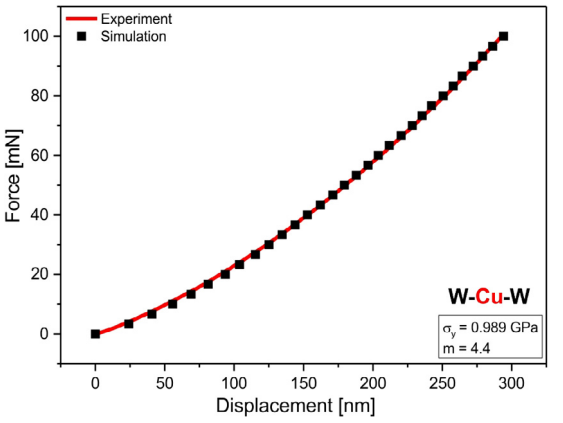

Fig. A.2. Experimental and fitted nanoindentation force–displacement curve for a W–Cu–W film.

Acknowledgements

Financial support by the Austrian Federal Government (in particular from the Bundesministerium für Verkehr, Innovation und Technologie and the Bundesministerium für Wissenschaft, Forschung und Wirtschaft) represented by Österreichische Forschungsförderungsgesellschaft mbH and the Styrian and the Tyrolean Provincial Government, represented by Steirische Wirtschaftsförderungsgesellschaft mbH and Standortagentur Tirol, within the framework of the COMET Funding Programme is gratefully acknowledged (837900). Furthermore, DK acknowledges financial support by the Austrian Science Fund FWF (project number P25325-N20).

Appendix A

The calculation of the flow behaviour of W and Cu is performed in two steps. First, the flow curve for a single nanoindent into a tungsten layer is recorded and then simulated (Fig. A.1). Using the Ramberg–Osgood material model, a yield strength of 1.97 GPa and an inverse hardening parameter of 14.3 are determined. Following, the stress–strain curve of tungsten is incorporated into the nanoindentation simulation of a W–Cu–W layer system and the flow curve for the copper layer is calculated to match the experiment (Fig. A.2). For the Cu layer the determined yield strength is 0.989 GPa and the inverse hardening parameter amounts to 4.4.

Appendix B

The initial idea for doing multiple cycles was to monitor the crack propagation with high resolution images after each cycle. Of course, an experiment with only one cycle could be paused after each crack extension for grabbing a high resolution image, but then a load relaxation caused by the compliance of the machine and possible thermal drift might influence the experiment. To make sure that we collect valid data we tested one sample (W–Cu–W S6) in a single loading to failure. As the geometries were slightly different, the force is converted to a normalized bending moment M and the displacement to an outer fibre strain ε using following equations to compare the results:

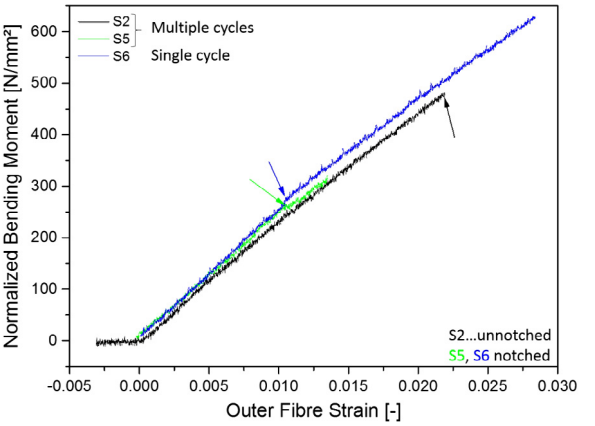

Fig. B.1. Loading curves for W–Cu–W samples S2 (unnotched, multiple cycles), S5 (notched, multiple cycles) and S6 (notched, single cycle).

$$M = \frac{FL}{BW(t)^2} \qquad \varepsilon = \frac{3x}{L^2}\frac{W(t)}{2}$$

F	Force
L	Bending length
B	Sample width
$W(t)$	Sample height—currentcrack length
x	Displacement

The loading curves converted with these two equations are plotted in Fig. B.1. The initial stiffness of all three samples is the same, as was to be expected. The arrows indicate the first crack propagation, where a reduction in stiffness is clearly visible. However, no differences between the static test and the cyclic experiments are evident. Based on these results we conclude that our approach of doing multiple cycles is valid, as within the limits of our experiment no influence of hardening due to the previous cycles is evident.

Please cite this article in press as: R. Treml, et al., Miniaturized fracture experiments to determine the toughness of individual films in a multilayer system, Extreme Mechanics Letters (2016), http://dx.doi.org/10.1016/j.eml.2016.01.004

Appendix C. Supplementary data

Supplementary material related to this article can be found online at http://dx.doi.org/10.1016/j.eml.2016.01.004.

References

[1] M. Sistaninia, O. Kolednik, Effect of a single soft interlayer on the crack driving force, Eng. Fract. Mech. 130 (2014) 21–41.
[2] E. Arzt, Size effects in materials due to microstructural and dimensional constraints: A comparative review, Acta Mater. 46 (1998) 5611–5626.
[3] A. Beaber, J. Nowak, O. Ugurlu, W. Mook, S. Girshick, R. Ballarini, W. Gerberich, Smaller is tougher, Phil. Mag. 91 (7–9) (2011) 1179–1189.
[4] B.N. Jaya, V. Jayaram, Fracture testing at small-length scales: From plasticity in Si to brittleness in Pt, JOM 68 (2016) 94–108.
[5] M.G. Mueller, V. Pejchal, G. Žagar, A. Singh, M. Cantoni, A. Mortensen, Fracture toughness testing of nanocrystalline alumina and fused quartz using chevron-notched microbeams, Acta Mater. 86 (2015) 385–395.
[6] S. Wurster, C. Motz, R. Pippan, Characterization of the fracture toughness of micro-sized tungsten single crystal notched specimens, Phil. Mag. 92 (14) (2012) 1803–1825.
[7] L. Zhang, H. Yang, X. Pang, K. Gao, A.A. Volinsky, Microstructure, residual stress, and fracture of sputtered TiN films, Surf. Coat. Technol. 224 (2013) 120–125.
[8] E. Weppelmann, M.V. Swain, Investigation of the stresses and stress intensity factors responsible for fracture of thin protective films during ultra-micro indentation tests with spherical indenters, Thin Solid Films 286 (1996) 111–121.
[9] M. Sebastiani, K.E. Johanns, E.G. Herbert, F. Carassiti, G.M. Pharr, A novel pillar splitting test for measuring fracture toughness of thin ceramic coatings, Phil. Mag. 95 (16–18) (2015) 1928–1944.
[10] B.N. Jaya, C. Kirchlechner, G. Dehm, Can microscale fracture tests provide reliable fracture toughness values? A case study in silicon, J. Mater. Res. 30 (5) (2015) 686–698.
[11] S. Massl, W. Thomma, J. Keckes, R. Pippan, Investigation of fracture properties of magnetron-sputtered TiN films by means of a FIB-based cantilever bending technique, Acta Mater. 57 (2009) 1768–1776.
[12] K. Matoy, H. Schönherr, T. Detzel, T. Schöberl, R. Pippan, C. Motz, G. Dehm, A comparative micro-cantilever study of the mechanical behvior of silicon based passivation films, Thin Solid Films 518 (2009) 247–256.
[13] M. Sebastiani, K. Johanns, E. Herbert, G. Pharr, Measurement of fracture toughness by nanoindentation methods: Recent advances and future challenges, Curr. Opin. Solid State Mater. Sci. 19 (2015) 324–333.
[14] J. Ast, T. Przybilla, V. Maier, K. Durst, M. Göken, Microcantilever bending experiments in NiAl—evaluation, size effects, and crack tip plasticity, J. Mater. Res. 29 (2014) 2129–2140.
[15] D. Armstrong, C. Hardie, J. Gibson, A. Bushby, P. Edmondson, S. Roberts, Small-scale characterisation of irradiated nuclear materials: Part II nanoindentation and micro-cantilever testing of ion irradiated nuclear materials, J. Nucl. Mater. 462 (2015) 374–381.
[16] M. Schlögl, C. Kirchlechner, J. Paulitsch, J. Keckes, P. Mayrhofer, Effects of structure and interfaces on fracture toughness of CrN/AlN multilayer coatings, Scr. Mater. 68 (2013) 917–920.
[17] A. Zeilinger, R. Daniel, M. Stefenelli, B. Sartory, L. Chitu, M. Burghammer, T. Schöberl, O. Kolednik, J. Keckes, C. Mitterer, Mechanical property enhancement in laminates through control of morphology and crystal orientation, J. Phys. D: Appl. Phys. 48 (2015).
[18] J. Rice, A path independent integral and the approximate analysis of strain concentration by notches and cracks, J. Appl. Mech. 35 (1968) 379–386.
[19] O. Kolednik, Fracture mechanics, in: Wiley Encyclopedia of Composites, John Wiley & Sons, Hoboken, New Yersey, USA, 2012, pp. 1126–1141.
[20] E. Hintsala, D. Kiener, J. Jackson, W. Gerberich, In-situ measurements of free-standing, ultra-thin film cracking in bending, Exp. Mech. 55 (2015) 1681–1690.
[21] N.K. Simha, F.D. Fischer, O. Kolednik, C.R. Chen, Inhomogeneity effects on the crack driving force in elastic and elastic–plastic materials, J. Mech. Phys. Solids 51 (2003) 209–240.
[22] H. Gao, B. Ji, I. Jäger, E. Arzt, P. Fratzl, Materials become insensitive to flaws at nanoscale: Lessons from nature, Proc. Natl. Acad. Sci. USA 100 (2003) 5597–5600.
[23] O. Kolednik, J. Predan, F. Fischer, P. Fratzl, Bioinspired design criteria for damage-resistant materials with periodically varying microstructure, Adv. Funct. Mater. 21 (2011) 3634–3641.
[24] R. Ritchie, The conflicts between strength and toughness, Nature Mater. 10 (2011) 817–822.
[25] R. Treml, D. Kozic, J. Zechner, X. Maeder, B. Sartory, H.-P. Gänser, R. Schöngrundner, J. Michler, R. Brunner, D. Kiener, Local determination of residual stress gradients in single- and multilayer thin film systems with high resolution, Acta Mater. 103 (2016) 616–623.
[26] S. Massl, J. Keckes, R. Pippan, A direct method of determining complex depth profiles of residual stresses in thin films on a nanoscale, Acta Mater. 55 (2007) 4835–4844.
[27] R. Schöngrundner, R. Treml, T. Antretter, D. Kozic, W. Ecker, D. Kiener, R. Brunner, Critical assessment of the determination of residual stress profiles in thin films by means of the ion beam layer removal method, Thin Solid Films 564 (2014) 321–330.
[28] S. Wurster, R. Treml, R. Fritz, M.W. Kapp, E. Langs, M. Alfreider, C. Ruhs, P.J. Imrich, G. Felber, D. Kiener, Novel methods for the site specific preparation of micromechanical structures, Pract Metallogr. 52 (2015) 131–146.
[29] D. Kiener, C. Motz, G. Dehm, R. Pippan, Overview on established and novel FIB based miniaturized mechanical testing using in-situ SEM, Int. J. Mater. Res. 100 (2009) 1074–1087.
[30] S. Pathak, S. Kalidindi, Spherical nanoindentation stress–strain curves, Mater. Sci. Eng. R 91 (2015) 1–36.
[31] J. Lubliner, Plasticity Theory, third ed., Dover Publications, New York, 2008, pp. 75–110.
[32] W. Ramberg, W. Osgood, Description of stress–strain curves by three parameters, Technical Note No. 902, National Advisory Committee For Aeronautics, Washington, DC, 1943.
[33] M.A. Hopcroft, W.D. Nix, T.W. Kenny, What is the Young's modulus of silicon, J. Microelectromech. Syst. 19 (2) (2010) 229–238.
[34] P.G. Sanders, J.A. Eastman, J.R. Weertman, Elastic and tensile behavior of nanocrystalline copper and palladium, Acta Mater. 45 (10) (1997) 4019–4025.
[35] E. Harry, A. Rouzaud, M. Ignat, P. Juliet, Mechanical properties of W and W(C) thin films: Young's modulus, fracture toughness and adhesion, Thin Solid Films 332 (1998) 195–201.
[36] E. Grünwald, R. Nuster, R. Treml, D. Kiener, G. Paltauf, R. Brunner, Young's modulus and Poisson's ratio characterization of tungsten thin films via laser ultrasound, Mater. Today: Proc. 2 (2015) 4289–4294.
[37] T. Anderson, Fracture Mechanics, third ed., CRC Press, Boca Raton, FL, 1995.
[38] N. Simha, F. Fischer, O. Kolednik, J. Predan, G. Shan, Crack tip shielding or anti-shielding due to smooth and discontinuous material inhomogeneities, Int. J. Fract. 135 (2005) 73–93.
[39] F. Iqbal, J. Ast, M. Göken, K. Durst, In situ micro-cantilever tests to study fracture properties of NiAl single crystals, Acta Mater. 60 (2012) 1193–1200.
[40] S. Liu, J. Wheeler, P. Howie, X. Zeng, J. Michler, W. Clegg, Measuring the fracture resistance of hard coatings, Appl. Phys. Lett. 102 (2013) 171907.
[41] D. Scheiber, V.I. Razumovskiy, P. Puschnig, R. Pippan, L. Romaner, Ab initio description of segregation and cohesion of grain boundaries in W-25 at.% Re alloys, Acta Mater. 88 (2015) 180–189.
[42] O. Kolednik, J. Predan, F. Fischer, Reprint of "Cracks in inhomogeneous materials: Comprehensive assessment using the configurational forces concept", Eng. Fract. Mech. 77 (2010) 3611–3624.
[43] O. Kolednik, R. Schöngrundner, F. Fischer, A new view on J-integrals in elastic–plastic materials, Int. J. Fract. 187 (2014) 77–107.
[44] O. Kolednik, J. Predan, F. Fischer, P. Fratzl, Improvements of strength and fracture resistance by spatial material property variations, Acta Mater. 68 (2014) 279–294.
[45] P. Fratzl, H. Gupta, F. Fischer, O. Kolednik, Hindered crack propagation in materials with periodically varying young's modulus—lessons from biological materials, Adv. Mater. 19 (2007) 2657–2661.

Please cite this article in press as: R. Treml, et al., Miniaturized fracture experiments to determine the toughness of individual films in a multilayer system, Extreme Mechanics Letters (2016), http://dx.doi.org/10.1016/j.eml.2016.01.004